Journal of Proteomes, Interactomes and Biological Networks

Article

HTT interactor network analysis for Huntington's disease: Integrating Predictive Tools, Structural Analysis, and Network Comparisons

Isaac Ambrogetti[1], Sofia Errigo[2], Guglielmo Gallo[3] and Emilia Giglio[4]

[1] Section of Genomics, Department of Pharmacy and Biotechnology, University of Bologna, 40138 Bologna, Italy; isaac.ambrogetti@studio.unibo.it
[2] Section of Genomics, Department of Pharmacy and Biotechnology, University of Bologna, 40138 Bologna, Italy; sofia.errigo2@studio.unibo.it
[3] Section of Genomics, Department of Pharmacy and Biotechnology, University of Bologna, 40138 Bologna, Italy; guglielmo.gallo@studio.unibo.it
[4] Section of Genomics, Department of Pharmacy and Biotechnology, University of Bologna, 40138 Bologna, Italy; emilia.giglio@studio.unibo.it

Abstract: Huntington's disease is a genetically inherited autosomal dominant neurodegenerative disorder, primarily associated with mutations in the polyQ residues found in the N-terminal domain of Huntingtin (HTT). Using machine-learning based tools for predicting the interaction sites, databases and visualization software, we aimed to get a better understanding of the protein interactome responsible for the disease and how it differs from the wild-type.

Throughout the research, we observed a notable disparity between the predicted interaction sites in the mHTT structure, which showed a significant increase compared to HTT's structure, and the experimental data and associated network, which showed the opposite result. It is therefore necessary to investigate more precisely the interactome of mHTT in HD with empirical experiments.

Keywords: Huntingtin, Huntington's disease, protein-protein interaction, interactome

1. Introduction

Huntingtin (HTT), a large and evolutionarily conserved scaffolding protein, has been the subject of intense studies in the past few decades due to its central role in both normal cellular functions and the pathogenesis of Huntington's disease (HD), a genetically inherited autosomal dominant neurodegenerative disorder. The pathological feature of HD is the loss of medium spiny neurons (MSN) in the striatum, and neurodegeneration spreads to other regions of the brain as the disease progresses. Clinically, HD is characterized by involuntary movement (chorea), cognitive decline, psychiatric disorders and dementia [1, 2].

With its ubiquitous expression and involvement in various cellular processes, HTT serves as a critical player in early embryonic development and continues to exert its influence throughout an organism's life. [3]

The HTT gene encodes a 348-kDa protein [4] and comprises 3142 residues (UniProt code: P42858) [2]. The CAG expansion at the 5′ end of the coding sequence of the HTT gene is a highly sensitive and specific marker for the inheritance of the mutation for Huntington's disease [5]. The CAG repeats result in the formation of a protein variant with an abnormal polyglutamine (polyQ) expansion in HTT. It is believed that the disease is caused by the gain of function of the mutant [3].

In unaffected people, the CAG sequence is repeated 10 to 29 times, with a higher likelihood of observing 17 or 19 triplets at the peak frequency [5], while a CAG expansion exceeding 35 repeats results in HD [4].

The very N-terminal region has been extensively studied. It is known to be preceded by 17 amino acids and followed by a proline-rich domain (PRD) [4].
The N-terminal 17 amino acids, conserved across vertebrates, form an amphipathic α-helix critical for endoplasmic reticulum retention and functioning as a nuclear export signal (NES).
The polyQ stretch, located immediately after the N-terminal 17 amino acids, is polymorphic in the human population. The expansion of the polyQ stretch has been linked to Huntington's disease and other neurodegenerative disorders: the consequences of the variability of the polyQ stretch on normal HTT function are not well understood yet, but it has been implicated in the regulation of autophagy and may have diverse consequences on HTT functions. [6]
The protein rich domain (PRD), specific to mammals and displaying variability in the non-HD population, is crucial for interactions with proteins that contain tryptophan (WW-proteins) or Src homology 3 (SH3) domains. [7]

The secondary structure analysis reveals that the first N-17 amino acids form an α-helical structure, while the polyQ stretch is a flexible region that can adopt several conformations including α-helix, random coil, and extended loop [3, 4, 8]. Therefore, the PRD's proline-proline helix, a relatively rigid structure, may stabilize the polyQ structure, influencing the aggregation propensity of mutant HTT [4].

Protein-protein interactions play a critical role in numerous cellular functions, and any dysfunction or disruption in these interactions has been associated with various pathological conditions [9]. HTT interacts with a wide range of proteins, contributing to the maintenance of an intracellular protein network and potentially playing essential roles in intracellular transportation. The exploration of proteins interacting with HTT holds significant importance, because mutations in HTT not only impact its own function but also affect the function of other interacting proteins [10].

With this study we aimed to find more information about the interactions of the Huntingtin protein, either in its wild type and mutated form, to unravel the complexities surrounding the protein. We conducted an investigation involving three key steps. Firstly, (i) we compared interaction sites predictions between the HTT and the mHTT seeking for incongruities, in order to uncover differences in protein-protein interaction patterns that could potentially play a role in the onset of HD. Subsequently, (ii) we made a comparative analysis of the known interactions between the two proteins, aiming to find some proteins specific to the mHTT. Lastly (iii), we compared the predicted interaction sites of the mHTT with the known interactors trying to identify some possible interaction site not yet annotated.

2. Materials and Methods

We used two huntingtin structures obtained via electron microscopy: PDB ID 6X9O [11, 12] and PDB ID 7DXJ [13,14], both in complex with huntingtin-associated protein 40 (HAP40).

BLAST (Basic Local Alignment Search Tool) [15] is a widely used bioinformatics tool that enables researchers to compare and analyze biological sequences. In the context of protein structure alignment, BLAST can be employed to identify similarities between the amino acid sequences of two proteins.

We used the online version of the tool to compare the sequences of the proteins 6X9O and 7DXJ, retrieved the required FASTA files from PDB [11, 13].

FATCAT (Flexible structure AlignmenT by Chaining Aligned fragment pairs allowing Twists) [16] is an approach that utilizes dynamic programming for flexible protein structure comparison. The structure alignment is defined as the AFPs (Aligned Fragment Pairs) chaining process, allowing at most n twists. The flexible structure alignment is converted into a rigid structure alignment when n is forced to be 0. We used the "Pairwaise alignment" function of the server to align and analyze the structures of the two protein structures of interest.

UCSF Chimera [17] is a highly versatile molecular visualization program used for interactive visualization and analysis of molecular structures and related data.
The protein structures of the proteins of interest were modeled using UCSF Chimera software. It was employed to compare the wild-type and mutant variants of the Huntingtin. The amino acid sequences of both the wild-type and mutant proteins were loaded into Chimera, and the structures were visualized side by side, after the removal of the chain B, corresponding to the HAP40. The "MatchMaker" tool in Chimera facilitated the alignment and superimposition of the two structures for comparative analysis. Structural differences arising from the mutation were identified and visualized using the previously performed FATCAT structural alignment, providing insights into the impact of the mutation on the protein's three-dimensional conformation.

ISPRED-SEQ [18] is a method that utilizes a deep-learning model for predicting the occurrence of Interaction Sites on a protein directly from its sequence. ISPRED-SEQ aims to enhance our understanding of protein functions by predicting regions involved in physical interactions between proteins.
We employed ISPRED-SEQ to comprehensively analyze the interactions of the Huntingtin protein. In the online version of the tool, we imported the two sequences in their FASTA format and displayed the results in an Excel file (see Supplementary File: ISPRED_SEQ_analysis.xlsx).

ISPRED4 (Interaction Site PREDictions, version 4) [19] is an improved structure-based predictor of protein-protein interaction sites on monomer surfaces. ISPRED4 is a machine-learning-based tool, and it incorporates features extracted from protein sequence and structure.
It has been run for both protein structures 6X9O and 7DXJ, importing as input the proteins in their PDB format. As result, we obtained predictions of the interaction sites of the proteins based on their structures, and the results were displayed in an Excel file (see Supplementary File: ISPREAD4_analysis.xlsx).

Cytoscape [20] is an open-source software platform used for visualizing, analyzing, and interpreting molecular interaction networks and biological pathways, providing also a basic set of features for data integration, analysis, and visualization. In addition to the basic features provided by the software itself, there are plugins, referred to as "Apps", which offer extended functionality for network and molecular profiling analyses, new layouts, additional file format support, scripting, and connection with databases.
Cytoscape software was employed for the comparative analysis of protein interaction networks between the wild-type and mutated form, by considering the Huntington's disease network. In order to obtain consistent results in the comparative process, we followed the same procedure for both the HTT and the mHTT: we imported the full STRING network in Cytoscape from the plugin StringApp [21], we set a threshold cutoff value of 0.6 and a maximum amount of protein of 2000 to display.

The network regarding the HTT has been imported as "Protein query", while the mutant one has been imported as "DISEASE query".
Once obtained the networks, the clustering process was performed using MCL [22], an algorithm provided by StringApp, applying a granularity parameter of 4, set as default.
The resulting network was then modified, choosing as parameter the visualization of only "physical subnetwork" to narrow the research of interest, and then clustered again to obtain a better visualization of the mHTT interactors, taking in consideration only the first neighbors.

IntAct [23] is an open-source database system and analysis tools for molecular interaction data. IntAct populates molecular interactions from experimentally-derived interaction data available in the published scientific literature and from direct scientists' submissions prior to publication in a peer-reviewed journal.
We identified relevant information about the binding sites between mHTT and its interactors by searching on the IntAct "Quick Search" tool, looking for the interactors found in the Huntington's disease network. Since the information found in the database does not concern mHTT directly but mostly involves interactions of HTT, the information that could not be retrieved using IntAct were found searching for scientific publications.

3. Results

The first structure of human huntingtin we used was obtained with cryoEM and has been released in 2020. This structure has an overall resolution of 2.60 Å (PDB ID: 6X9O) [11].
The other structure we used was still obtained with cryoEM and has been released in 2021. It has an overall resolution of 3.60 Å (PDB ID: 7DXJ) [13].

3.1. Alignment of the two structures

3.1.1. Amino acids sequences alignment using BLAST

Considering the alignment of the two sequences using BLAST [15], we noticed that the first sequence (6X9O) has a length of 3156 amino acids, while the other (7DXJ) has a length of 3167 amino acids. The alignment revealed a high degree of similarity between the two sequences, with an overall identity of 99%. However, while the overall sequence remains highly conserved, a distinctive divergence was identified in the polyglutamine region. The polyQ region in 6X9O showed the presence of 18 glutamine (Q) repeats, whereas in 7DXJ there were 40 glutamine repeats. This significant difference indicates a mutant form of the protein, suggesting a potential association with Huntington's Disease (HD). (see Supplementary File: BLAST_alignment.txt).

3.1.2. Proteins structural alignment using FATCAT and Chimera

We proceed with the structural alignment of the two sequences using FATCAT [16] and Chimera [17].
The structural alignment on FATCAT revealed that there is not a substantial difference in initial-RMSD and optimal-RMSD (1.40 and 1.48 respectively). Furthermore, both Identity and Similarity have high scores (97.50% and 97.62% respectively). These results show that the two proteins seem very similar, which is probably due to the absence of the structure of the polyQ tail in both pdb files (see Supplementary File: FATCAT_alignment.txt).
In Chimera we had been able to visualize the protein structure and it has been possible to visually and formally detect the gaps in the structure detection (see Figure 1), which

corresponded to the gap sites on FATCAT too, since they both refer to the PDB file which contain the information about the protein structure.

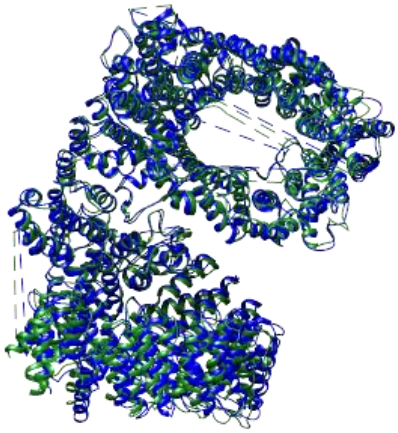

Figure 1. Superimposition of 6X9O (green) and 7DXJ (blue) proteins using Chimera (see text for details). The dashed lines represent the missing connections due to the lack on information of the actual structure in PDB.

3.2 Prediction interaction sites

3.2.1 ISPRED-SEQ

From the result of the run of ISPREAD-SEQ on our proteins of interest (see Supplementary File: ISPRED_SEQ_analysis.xlsx), we noticed that there are amino acids in which the interaction site is predicted in just one of the two proteins; the threshold value used to predict an interaction site is 0.5. We had a look at the differences in probabilities of having an interaction site to see if there could be significant results. We considered a change in the probability of being an interaction site significant when the absolute value of the differences was greater than 0.1.

We obtained two most relevant patches of amino acids, respectively at the positions 786:793 (ref. 6X9O in ISPREAD_SEQ_analysis.xlsx) and 2358:2370 (ref. 6X9O in ISPREAD_SEQ_analysis.xlsx). The first one shows a predicted interaction site in the mHTT that is not present in the HTT, while the second one exhibits a predicted interaction site in the HTT not present in the mHTT.

3.2.2 ISPRED4

In order to have a better understanding of how interaction sites are placed on the proteins we repeated the analysis done with ISPRED-SEQ, using ISPRED4 (see Supplementary File: ISPRED4_analysis).

The analysis on ISPRED4 showed us that the number of predicted interfaces in 6X9O (HTT) is 192, whereas in 7DXJ (mHTT) this number doubles to 394. In this analysis we used a threshold of 0.7 for considering relevant a variation in the prediction of the interaction sites, and we choose the patches having a length of at least 7 amino acids.

We found five patches showing predicted binding sites only in 7DXJ and not in 6X9O: 104:113, 295:310, 705:711, 790:799, 2238:2244 patch correspondence on the 6X9O aa sequence.

There were no relevant patches found present only in 6X9O and not in 7DXJ.

3.3 Comparison analysis of HTT and mHTT network interactors

We obtained networks of the HTT and mHTT, resulting respectively in 37 nodes (see Figure 2.a) and 6 nodes (see Figure 2.b). In the latter, we found HYPK, ZDHHC17, ZDHHC13, RASD2, and the coding genes for the HAP40: F8A1, F8A2 (see Figure 2.b).
Lastly, we compared the network obtained, excluding all the nodes present in the HTT network from the mHTT one, resulting in just one remaining node: RASD2.

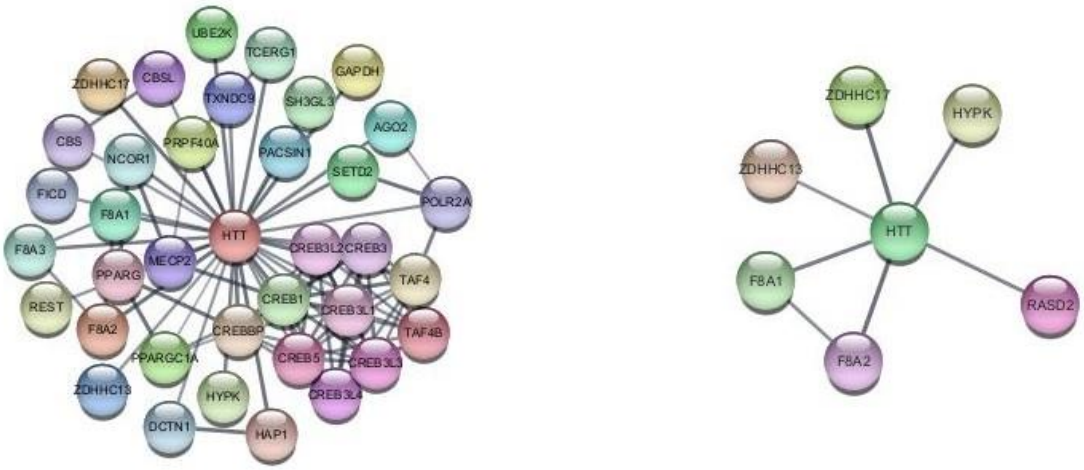

(a) **(b)**

Figure 2. (a) Network of direct interactions of the Huntingtin protein. The network was obtained using Cytoscape (see text for details). The node in the middle corresponds to the HTT and all the other nodes connected are the first neighbors of the protein of interest. (b) Network of direct interactions of mHTT in the Huntington disease. The network was obtained using Cytoscape (see text for details). The node in the middle corresponds to the mHTT and all the other nodes connected are the first neighbors of the protein of interest.

3.4 Analysis of interaction sites using IntAct and online literature

Throughout our analysis on IntAct we identified relevant information about the binding sites between mHTT and two out of six interactors we found in the HD's network on Cytoscape.
Specifically, there is evidence that HYPK binds in the region 18:38 of a mutated HTT protein with a polyQ of 55 glutamines [24] and ZDHHC17 binds in the region 1:500 of a mHTT with a polyQ of 49 glutamines [25].
For F8A1/2 it has been proved that it binds HTT around position 1:504 and, since we found evidence that the length of the polyQ of our protein of interest does not alter the binding of the HAP40 [12], we can infer that it binds the mHTT also in the same region.
Furthermore, ZDHCC13, responsible for protein S-palmitoylation, has been linked to HD through research, indicating that its deficit could be linked to HD [26].
RASD2 [27] stands out prominently within the network of interactors, as it is the only candidate for which we have a binding present in the mutated form of the protein. However, literature on the binding of RASD2 with Huntingtin is limited and it's still unknown the specific binding site. Research has nevertheless demonstrated its crucial role in the movement and transportation of the HD protein, mHTT, via tunneling nanotube (TNT). Notably, the deletion of Rhes, a GTP-binding protein encoded by RASD2, has been demonstrated to hinder the efficient transport of mHTT within the striatum and from the striatum to cortical areas in the brain [28]. This emphasizes the role of RASD2 in facilitating the movement and transfer of mHTT between neurons and different brain regions.

4. Discussion

Comparing the outcome of BLAST [15] with the results retrieved from Chimera [17] and FATCAT [16] analyses, we noticed that the amino acid sequences correspond consistently between the wild-type HTT and its mutated form. This alignment persisted, even in regions where the Chimera and FATCAT results exhibited no correlation, primarily due to the absence of experimentally confirmed secondary structure information (see Figure 1). This observation suggests that, beyond the regions with unavailable structural data, HTT and mHTT exhibit similar structural characteristics. Notably, the main distinguishing factor between HTT and mHTT is the expanded polyglutamine tract within the N-terminal domain.

Our analysis then delved into the predictions of interaction sites using ISPRED-SEQ [18] and ISPRED4 [19]. In both the analyses we observed more predicted interaction in the mHTT, suggesting potential alterations in interaction profiles due to the polyQ expansion in mHTT. Moreover, ISPRED4 displayed a twofold increase in the interfaces predicted in the 7DXJ, supporting the hypothesis that the mutated form indeed exhibits a more complex interaction network. The structural alterations induced by the expanded polyglutamine tract likely contribute to the creation of novel interaction sites, reflecting the intricate molecular consequences of the mutation [29].

Expanding our focus to the protein interaction networks, the comparative analysis using Cytoscape [20] revealed substantial differences in the interactors of HTT and mHTT. The mHTT network exhibited fewer nodes but included specific proteins absent in the HTT network (see Figure 2).

It's noteworthy that this result seems to be in contrast with the predictions of ISPRED-SEQ [18] and ISPRED4 [19], which suggested an increased number of interaction sites in the mutated form. This discrepancy could be due to the fact that experimental data for mHTT in databases like IntAct [23] might be relatively limited.

Simultaneously, our examination of the IntAct [23] database provided valuable insights on known interactions. However, the absence of known interactions in specific regions such as around the eight hundredth amino acid, despite its high probability of being an interaction site, signals an area that demands further experimental examination.

5. Conclusions

As well established, the length of the polyQ tail in the Huntingtin is the main determinant of the disease development. In our analysis we confirmed that HTT and mHTT, differing only in the N-terminal domain, are able to form networks with different interactors. Predictive tools indicated an increased number of interaction sites in mHTT. Nevertheless, accurate documented interactions of these proteins are difficult to find also in well-structured databases such as IntAct, leading to network representations which show different information from the predicted ones.

Therefore, further structural and functional analysis are needed to delineate the molecular consequences of polyQ expansion and its implications for the pathophysiology of Huntington's disease.

Supplementary Materials: The following supporting information can be found attached to the report: ISPRED4_analysis.xlsx, ISPRED_SEQ_analysis.xlsx, BLAST_alignment.txt, FATCAT_alignment.txt.

[1] L. Liu *et al.*, 'Huntingtin Interacting Proteins and Pathological Implications', *Int. J. Mol. Sci.*, vol. 24, no. 17, p. 13060, Aug. 2023, doi: 10.3390/ijms241713060.

[2] 'HTT - Huntingtin - Homo sapiens (Human) | UniProtKB | UniProt'. Accessed: Feb. 04, 2024. [Online]. Available: https://www.uniprot.org/uniprotkb/P42858/entry

[3] G. Babbi, C. Savojardo, P. L. Martelli, and R. Casadio, 'Huntingtin: A Protein with a Peculiar Solvent Accessible Surface', *Int. J. Mol. Sci.*, vol. 22, no. 6, Art. no. 6, Jan. 2021, doi: 10.3390/ijms22062878.

[4] F. Saudou and S. Humbert, 'The Biology of Huntingtin', *Neuron*, vol. 89, no. 5, pp. 910–926, Mar. 2016, doi: 10.1016/j.neuron.2016.02.003.

[5] B. Kremer *et al.*, 'A Worldwide Study of the Huntington's Disease Mutation: The Sensitivity and Specificity of Measuring CAG Repeats', *N. Engl. J. Med.*, vol. 330, no. 20, pp. 1401–1406, May 1994, doi: 10.1056/NEJM199405193302001.

[6] S. Zheng, E. B. D. Clabough, S. Sarkar, M. Futter, D. C. Rubinsztein, and S. O. Zeitlin, 'Deletion of the huntingtin polyglutamine stretch enhances neuronal autophagy and longevity in mice', *PLoS Genet.*, vol. 6, no. 2, p. e1000838, Feb. 2010, doi: 10.1371/journal.pgen.1000838.

[7] P. Harjes and E. E. Wanker, 'The hunt for huntingtin function: interaction partners tell many different stories', *Trends Biochem. Sci.*, vol. 28, no. 8, pp. 425–433, Aug. 2003, doi: 10.1016/S0968-0004(03)00168-3.

[8] M. W. Kim, Y. Chelliah, S. W. Kim, Z. Otwinowski, and I. Bezprozvanny, 'Secondary structure of Huntingtin amino-terminal region', *Struct. Lond. Engl. 1993*, vol. 17, no. 9, pp. 1205–1212, Sep. 2009, doi: 10.1016/j.str.2009.08.002.

[9] E. Martino, S. Chiarugi, F. Margheriti, and G. Garau, 'Mapping, Structure and Modulation of PPI', *Front. Chem.*, vol. 9, p. 718405, 2021, doi: 10.3389/fchem.2021.718405.

[10] E. E. Wanker, A. Ast, F. Schindler, P. Trepte, and S. Schnoegl, 'The pathobiology of perturbed mutant huntingtin protein–protein interactions in Huntington's disease', *J. Neurochem.*, vol. 151, no. 4, pp. 507–519, 2019, doi: 10.1111/jnc.14853.

[11] R. P. D. Bank, 'RCSB PDB - 6X9O: High resolution cryoEM structure of huntingtin in complex with HAP40'. Accessed: Feb. 04, 2024. [Online]. Available: https://www.rcsb.org/structure/6X9O

[12] B. Huang *et al.*, 'Pathological polyQ expansion does not alter the conformation of the Huntingtin-HAP40 complex', *Struct. Lond. Engl. 1993*, vol. 29, no. 8, pp. 804-809.e5, Aug. 2021, doi: 10.1016/j.str.2021.04.003.

[13] R. P. D. Bank, 'RCSB PDB - 7DXJ: Human 46QHuntingtin-HAP40 complex structure'. Accessed: Feb. 04, 2024. [Online]. Available: https://www.rcsb.org/structure/7DXJ

[14] R. J. Harding *et al.*, 'Huntingtin structure is orchestrated by HAP40 and shows a polyglutamine expansion-specific interaction with exon 1', *Commun. Biol.*, vol. 4, no. 1, Art. no. 1, Dec. 2021, doi: 10.1038/s42003-021-02895-4.

[15] S. F. Altschul, W. Gish, W. Miller, E. W. Myers, and D. J. Lipman, 'Basic local alignment search tool', *J. Mol. Biol.*, vol. 215, no. 3, pp. 403–410, Oct. 1990, doi: 10.1016/S0022-2836(05)80360-2.

[16] Y. Ye and A. Godzik, 'FATCAT: a web server for flexible structure comparison and structure similarity searching', *Nucleic Acids Res.*, vol. 32, no. Web Server issue, pp. W582-585, Jul. 2004, doi: 10.1093/nar/gkh430.

[17] E. F. Pettersen *et al.*, 'UCSF Chimera--a visualization system for exploratory research and analysis', *J. Comput. Chem.*, vol. 25, no. 13, pp. 1605–1612, Oct. 2004, doi: 10.1002/jcc.20084.

[18] M. Manfredi, C. Savojardo, P. L. Martelli, and R. Casadio, 'ISPRED-SEQ: Deep Neural Networks and Embeddings for Predicting Interaction Sites in Protein Sequences', *J. Mol. Biol.*, vol. 435, no. 14, p. 167963, Jul. 2023, doi: 10.1016/j.jmb.2023.167963.

[19] C. Savojardo, P. Fariselli, P. L. Martelli, and R. Casadio, 'ISPRED4: interaction sites PREDiction in protein structures with a refining grammar model', *Bioinforma. Oxf. Engl.*, vol. 33, no. 11, pp. 1656–1663, Jun. 2017, doi: 10.1093/bioinformatics/btx044.

[20] P. Shannon *et al.*, 'Cytoscape: a software environment for integrated models of biomolecular interaction networks', *Genome Res.*, vol. 13, no. 11, pp. 2498–2504, Nov. 2003, doi: 10.1101/gr.1239303.

[21] N. T. Doncheva, J. H. Morris, J. Gorodkin, and L. J. Jensen, 'Cytoscape StringApp: Network Analysis and Visualization of Proteomics Data', *J. Proteome Res.*, vol. 18, no. 2, pp. 623–632, Feb. 2019, doi: 10.1021/acs.jproteome.8b00702.

[22] 'Markov Clustering (MCL): a cluster algorithm for graphs'. Accessed: Feb. 04, 2024. [Online]. Available: https://hpc.nih.gov/apps/mcl.html

[23] S. Orchard *et al.*, 'The MIntAct project--IntAct as a common curation platform for 11 molecular interaction databases', *Nucleic Acids Res.*, vol. 42, no. Database issue, pp. D358-363, Jan. 2014, doi: 10.1093/nar/gkt1115.

[24] L. S. Kaltenbach *et al.*, 'Huntingtin Interacting Proteins Are Genetic Modifiers of Neurodegeneration', *PLoS Genet.*, vol. 3, no. 5, p. e82, May 2007, doi: 10.1371/journal.pgen.0030082.

[25] S. L. Butland *et al.*, 'The palmitoyl acyltransferase HIP14 shares a high proportion of interactors with huntingtin: implications for a role in the pathogenesis of Huntington's disease', *Hum. Mol. Genet.*, vol. 23, no. 15, pp. 4142–4160, Aug. 2014, doi: 10.1093/hmg/ddu137.

[26] E. Napoli *et al.*, 'Zdhhc13-dependent Drp1 S-palmitoylation impacts brain bioenergetics, anxiety, coordination and motor skills', *Sci. Rep.*, vol. 7, no. 1, Art. no. 1, Oct. 2017, doi: 10.1038/s41598-017-12889-0.

[27] U. N. Ramírez-Jarquín, M. Sharma, N. Shahani, Y. Li, S. Boregowda, and S. Subramaniam, 'Rhes protein transits from neuron to neuron and facilitates mutant huntingtin spreading in the brain', *Sci. Adv.*, vol. 8, no. 12, p. eabm3877, Mar. 2022, doi: 10.1126/sciadv.abm3877.

[28] Y. Pan, B. Tang, X.-J. Li, S. Li, and Q. Liu, 'Rhes depletion promotes striatal accumulation and aggregation of mutant huntingtin in a presymptomatic HD mouse model', *Front. Aging Neurosci.*, vol. 15, p. 1237018, 2023, doi: 10.3389/fnagi.2023.1237018.

[29] C. Gopalakrishnan, S. Jethi, N. Kalsi, and R. Purohit, 'Biophysical Aspect of Huntingtin Protein During polyQ: An In Silico Insight', *Cell Biochem. Biophys.*, vol. 74, no. 2, pp. 129–139, Jun. 2016, doi: 10.1007/s12013-016-0728-7.